ISSN 1674-1056
http://cpb.iphy.ac.cn
http://iopscience.iop.org/cpb
中国物理 B
Chinese Physics
中国物理
Chinese Physics B

Compressed ghost imaging based on differential speckle patterns

Le Wang(王乐), Shengmei Zhao(赵生妹)
Citation: Chin. Phys. B . 2020, 29(2): 024204 . **doi:** 10.1088/1674-1056/ab671a
Journal homepage: http://cpb.iphy.ac.cn; http://iopscience.iop.org/cpb

What follows is a list of articles you may be interested in

Experimental demonstration of influence of underwater turbulence on ghost imaging

Man-Qian Yin(殷曼倩), Le Wang(王乐), Sheng-Mei Zhao(赵生妹)
Chin. Phys. B . 2019, 28(9): 094201 . **doi:** 10.1088/1674-1056/ab33ee

Mask-based denoising scheme for ghost imaging

Yang Zhou(周阳), Shu-Xu Guo(郭树旭), Fei Zhong(钟菲), Tian Zhang(张天)
Chin. Phys. B . 2019, 28(8): 084204 . **doi:** 10.1088/1674-1056/28/8/084204

Enhancement of spatial resolution of ghost imaging via localizing and thresholding

Yunlong Wang(王云龙), Yingnan Zhou(周英男), Shaoxiong Wang(王少雄), Feiran Wang(王斐然), Ruifeng Liu(刘瑞丰), Hong Gao(高宏), Pei Zhang(张沛), Fuli Li(李福利)
Chin. Phys. B . 2019, 28(4): 044202 . **doi:** 10.1088/1674-1056/28/4/044202

Reflective ghost imaging free from vibrating detectors

Heng-xing Li(李恒星), Yan-feng Bai(白艳锋), Xiao-hui Shi(施晓辉), Su-qin Nan(南苏琴), Li-jie Qu(屈利杰), Qian Shen(沈倩), Xi-quan Fu(傅喜泉)
Chin. Phys. B . 2017, 26(10): 104204 . **doi:** 10.1088/1674-1056/26/10/104204

Optical encryption scheme based on ghost imaging with disordered speckles

Yu-dong Zhang(张玉东), Sheng-mei Zhao(赵生妹)
Chin. Phys. B . 2017, 26(5): 054205 . **doi:** 10.1088/1674-1056/26/5/054205

Compressed ghost imaging based on differential speckle patterns*

Le Wang(王乐)[1] and Shengmei Zhao(赵生妹)[1,2,†]

[1] Institute of Signal Processing and Transmission, Nanjing University of Posts and Telecommunications (NUPT), Nanjing 210003, China
[2] Key Laboratory of Broadband Wireless Communication and Sensor Network Technology (NUPT), Ministry of Education, Nanjing 210003, China

(Received 21 October 2019; revised manuscript received 17 November 2019; accepted manuscript online 3 January 2020)

We propose a compressed ghost imaging scheme based on differential speckle patterns, named CGI-DSP. In the scheme, a series of bucket detector signals are acquired when a series of random speckle patterns are employed to illuminate an unknown object. Then the differential speckle patterns (differential bucket detector signals) are obtained by taking the difference between present random speckle patterns (present bucket detector signals) and previous random speckle patterns (previous bucket detector signals). Finally, the image of object can be obtained directly by performing the compressed sensing algorithm on the differential speckle patterns and differential bucket detector signals. The experimental and simulated results reveal that CGI-DSP can improve the imaging quality and reduce the number of measurements comparing with the traditional compressed ghost imaging schemes because our scheme can remove the environmental illuminations efficiently.

Keywords: ghost imaging, compressed sensing, differential speckle patterns, differential bucket detector signals

PACS: 42.30.Va, 42.30.Wb **DOI:** 10.1088/1674-1056/ab671a

1. Introduction

Ghost imaging (GI) is a special optical imaging scheme,[1–7] where one of the two spatially correlated optical beams illuminates an object and is detected by a bucket detector without any spatial resolution, and the other beam is measured by a spatially resolving detector or computing offline. Then the object could be imaged by correlating the speckle patterns and corresponding bucket detector signals. However, the number of measurements are required much more to obtain a clear image. Subsequently, compressed ghost imaging (CGI)[8] was proposed to obtain a high quality image of object by exploiting the compressed sensing (CS)[9] algorithm from far fewer measurements than what is usually considered necessary in traditional GI schemes. CS can be used in CGI to reduce both the acquisition time and the number of measurement significantly by the aid of the redundant structure of the images. Since then, CGI has been received much attention and considerable number of methods and applications based on CGI has been proposed.[10–14]

However, the imaging quality of CGI is susceptible to the environmental illuminations. Complementary CGI (CCGI)[15] is proposed to solve this issue, which uses the complementary speckle pattern pairs[16,17] consisting of the speckle pattern and its inverse speckle pattern to illuminate the object and then acquire the differential signals by taking the difference among two bucket detector signals corresponding to the speckle pattern and its inverse speckle pattern. Instead of the bucket detector signals, the differential signals are used to reconstruct the images. Due to the inference of environmental illuminations can be removed efficiently in the differential signals, the image quality can be dramatically improved. However, the number of measurement of this method is large, which is twice as much as the traditional CGI (TCGI).

In this paper, we present a compressed ghost imaging scheme based on differential speckle patterns, named CGI-DSP. In the scheme, a series of bucket detector signals are acquired when an unknown object is illuminated by a series of random speckle patterns, and then the differential speckle patterns (differential bucket detector signals) are obtained by taking the difference between present random speckle patterns (present bucket detector signals) and previous random speckle patterns (previous bucket detector signals). Finally, the image of object can be obtained directly by performing the compressed sensing algorithm on the differential speckle patterns and differential bucket detector signals. The advantage of the CGI-DSP scheme is that the number of measurements could be reduced and the imaging quality can be improved comparing with traditional CGI (TCGI) and complementary CGI (CCGI).

The remainder of the paper is arranged as follows. CGI-DSP is presented in Section 2. In Section 3, the performance of CGI-DSP is discussed by simulations and experiments. Finally, the paper is concluded by Section 4.

2. Scheme description

The schematic diagram of the CGI-DSP is shown in Fig. 1. A series of random speckle patterns $I_i(x,y)$ are produced from the light source and then are modulated by a

*Project supported by the National Natural Science Foundation of China (Grant Nos. 11847062 and 61871234), the Natural Science Foundation of Jiangsu Province, China (Grant No. BK20180755), and the Science Fund from NUPT (Grant No. NY218098).

†Corresponding author. E-mail: zhaosm@njupt.edu.cn

© 2020 Chinese Physical Society and IOP Publishing Ltd

digital micro-mirror device (DMD), where i represents the i-th speckle pattern, the resolution of the speckle pattern is $N_x \times N_y$, the value of speckle pattern for each coordinate (x,y) is either white 1 or black 0, and $x = 1,\ldots,N_x$; $y = 1,\ldots,N_y$; $N = N_x \times N_y$. Additionally, the ratio of white value 1 and black value 0 of each speckle pattern is close to 1 : 1.

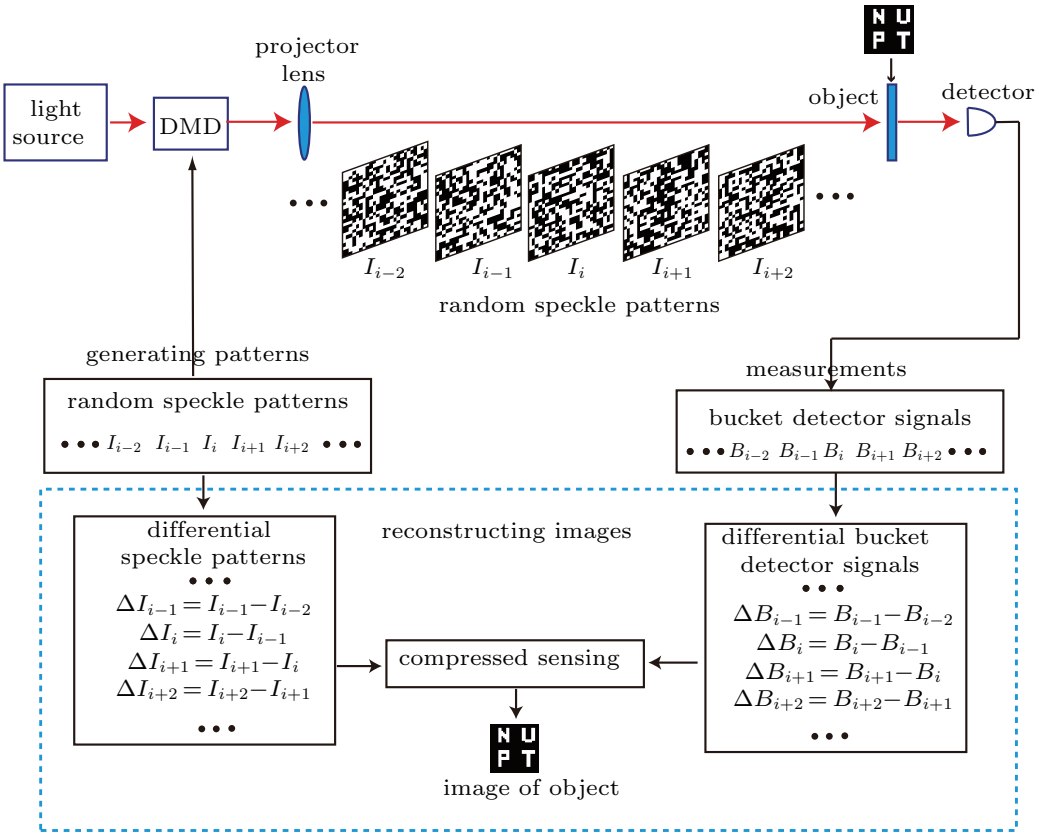


Fig. 1. A schematic diagram of the CGI-DSP scheme.

The speckle pattern $I_i(x,y)$ interacts with an object through a projector lens and then is measured by a bucket detector to get a bucket detector signal B_i,

$$B_i = \eta \int I_i(x,y)T(x,y)\mathrm{d}x\mathrm{d}y + n, \tag{1}$$

where n is the noise from environmental illuminations, $T(x,y)$ represents the distribution function of the object, and η represents the responsivity of bucket detector.

Furthermore, we can obtain a differential speckle pattern, $\Delta I_i(x,y)$, by taking the difference between present random speckle patterns $I_i(x,y)$ and previous random speckle patterns $I_{i-1}(x,y)$,

$$\Delta I_i(x,y) = I_i(x,y) - I_{i-1}(x,y). \tag{2}$$

Due to the ratio of white value 1 and black value 0 of each speckle pattern is close to 1 : 1, it is found that the values of $\Delta I_i(x,y)$ are -1, 0, and $+1$, and the values of $\Delta I_i(x,y)$ satisfy the characteristics of statistical distribution,[18]

$$\Delta I_i(x,y) = \begin{cases} -1 & \text{with probability } 1/4, \\ 0 & \text{with probability } 1/2, \\ +1 & \text{with probability } 1/4. \end{cases} \tag{3}$$

Thus the differential speckle patterns, $\Delta I_i(x,y)$, are sparse random and satisfies the Johnson–Lindenstrauss lemma.[19] It has the advantages of no floating point arithmetic and easy to compute because half of the computation could be avoided.[18]

Therefore, a differential bucket detector signal ΔB_i between the present bucket detector signal B_i and the previous bucket detector signals B_{i-1} is

$$\Delta B_i = B_i - B_{i-1} = \eta \int \Delta I_i(x,y)T(x,y)\mathrm{d}x\mathrm{d}y. \tag{4}$$

Thus we can see that the noises from the environmental illuminations n could be eliminated efficiently.

Above steps are repeated M to accumulate M random speckle patterns $\{I_i(x,y)\}_{i=0}^{M-1}$ and their corresponding bucket detector signals $\{B_i\}_{i=0}^{M-1}$. Therefore, $M-1$ differential speckle patterns $\{\Delta I_i(x,y)\}_{i=1}^{M-1}$ and their corresponding differential bucket detector signal $\{\Delta B_i\}_{i=1}^{M-1}$ are acquired.

Finally, the image of object is reconstructed by compressed sensing algorithm.[8] Here, TVAL3 algorithm[20] is used, which has the advantage of the reconstruction of a quality image. Therefore, the object's image $\hat{T}(x,y)$ can be recon-

structed by

$$\min \sum_j \|D_j \boldsymbol{T}\|_1 + \frac{\mu}{2}\|\boldsymbol{B} - \boldsymbol{A}\boldsymbol{T}\|_2^2, \tag{5}$$

where $\boldsymbol{B}$ is an $(M-1)\times 1$ vector containing $M-1$ differential bucket detector signals $\{\Delta B_i\}_{i=1}^{M-1}$. $\boldsymbol{T}$ is an $N\times 1$ vector by reforming the two-dimensional (2D) reconstructed image $\hat{T}(x,y)$, whose discrete gradient at element j ($j=1,2,\ldots,N$) is denoted as $D_j\boldsymbol{T}$. $\boldsymbol{A}$ is an $(M-1)\times N$ matrix consisting of $M-1$ differential speckle patterns $\{\Delta I_i(x,y)\}_{i=1}^{M-1}$, where each $1\times N$ row vector is reshaped from a two-dimensional differential speckle pattern $\Delta I_i(x,y)$. μ is a coefficient to balance data fidelity and regularization which is set as 2^{12} in this paper.

3. Result and discussion

We discuss the performance of the CGI-DSP scheme by experiments and numerical simulations in this section.

The experimental system of CGI-DSP is shown in Fig. 2. A DMD (TI DLPC350) modulates the light from a red LED to generate a series of the binary random speckle pattern $I_i(x,y)$. The speckle patterns are then projected by a lens onto an object. Subsequently, the reflective light goes through a bandpass filter (633 nm) and then is measured by a bucket detector (Thorlabs PMM02). Then detection results B_i are recorded by a computer records via an ADC (NI USB-6341). Finally, the compressed sensing algorithm is used to reconstruct the images of the object by using the differential speckle patterns $\Delta I_i(x,y)$ and the differential bucket detector signal ΔB_i. In addition, we use another LED as a background light source, where the LED is driven by a arbitrary waveform generator to generate the light with a sinusoidal intensity. The frequency of the sinusoidal intensity light equals to $1/10$ times the frequency of speckle patterns generation.

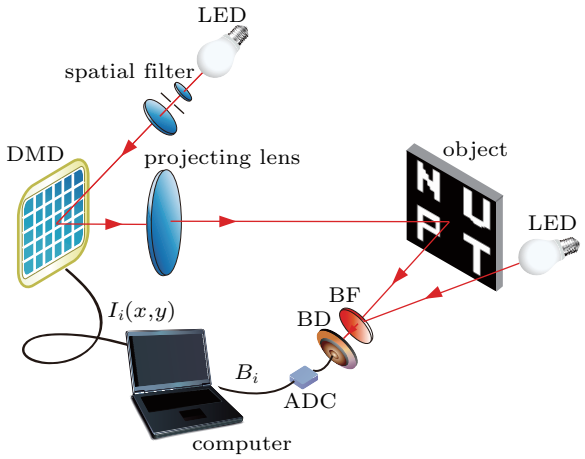


Fig. 2. A schematic diagram of the CGI-DSP scheme experimental system. DMD: digital micro-mirror device; BF: bandpass filter; BD: bucket detector, and ADC: analogue-to-digital converter.



Fig. 3. The numerical simulation results of the "NUPT" logo by using CGI-DSP scheme, where MSE is presented together.



Fig. 4. The numerical simulation results of the "NUPT" logo by using CCGI scheme, where MSE is presented together.



Fig. 5. The numerical simulation results of the "NUPT" logo by using TCGI scheme, where MSE is presented together.

Additionally, mean square error (MSE) is used to evaluate the imaging quality quantitatively,[14]

$$\mathrm{MSE} = \frac{1}{N_x \times N_y} \sum_{x,y} (\hat{T}(x,y) - T(x,y))^2, \tag{6}$$

where $\hat{T}(x,y)$ and $T(x,y)$ are the distribution functions of the recovered image and the original image, respectively.

To verify the feasibility of CGI-DSP, we first perform the numerical simulations, and compare the results of CGI-DSP with those results using CCGI and TCGI with different number of measurements and SNRs, which are shown in Figs. 3–5. Here we use 64×64-pixels binary random speckle patterns to illuminate the object.

The simulated results shown in Figs. 3–5 are from only one realization. We can find that with the increase of the number of measurements and SNRs, the reconstructed images have an obvious trend to be clearer and corresponding MSEs trend to be smaller for CGI-DSP, CCGI, and TCGI. But MSEs of reconstructed images do not monotonically decrease with the increase of SNRs because of the fluctuations of noise. However, images recovered by CGI-DSP trend to be better and corresponding MSEs trend to be smaller comparing to the images reconstructed by using CCGI and TCGI when the number of measurements and SNR are the same, because CGI-DSP has the ability of improving the imaging quality.

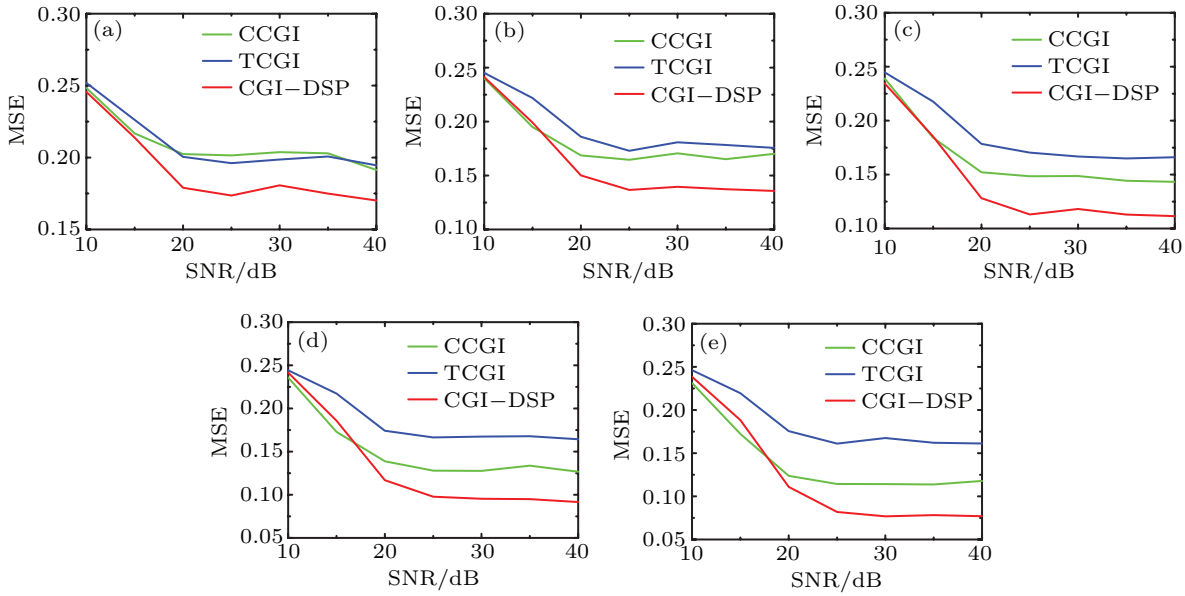


Fig. 6. The numerical simulation results of reconstructed the "NUPT" logo images' MSEs as a function of the SNRs for CGI-DSP, CCGI, and TCGI, where panel (a)–(e) are results when the numbers of measurements are 164, 328, 492, 655, 819, respectively.



Fig. 7. The experimental results of the "NUPT" logo by using CGI-DSP scheme, where MSE is presented together.

Furthermore, the performance of reconstructed images' MSE as a function of the SNR for CGI-DSP, CCGI, and TCGI is shown in Fig. 6, where figures 6(a)–6(e) are results when the numbers of measurements are 164, 328, 492, 655, 819, respectively. All the MSEs are the average of 100 simulated results. It is found that the larger the SNR, the better the image quality and the smaller the MSE. Moveover, the MSEs of CGI-DSP are smaller than those of CCGI and TCGI with the increase of SNR.

In addition, we perform the experiments and the results are shown in Figs. 7–9, where the object is the "NUPT" logo. Here we use 64×64-pixels binary random speckle patterns to illuminate the object. It is seen that the experimental results are similar to simulated results shown in Figs. 3–6, where with the increase of the number of measurements, the images recovered by CGI-DSP are clearer and the corresponding MSEs are smaller comparing with CCGI and TCGI. When images recovered by three schemes under the same condition of the number of measurements, the imaging quality of CGI-DSP is better than that of CCGI and TCGI because CGI-DSP could improve the imaging quality comparing with CCGI and TCGI.

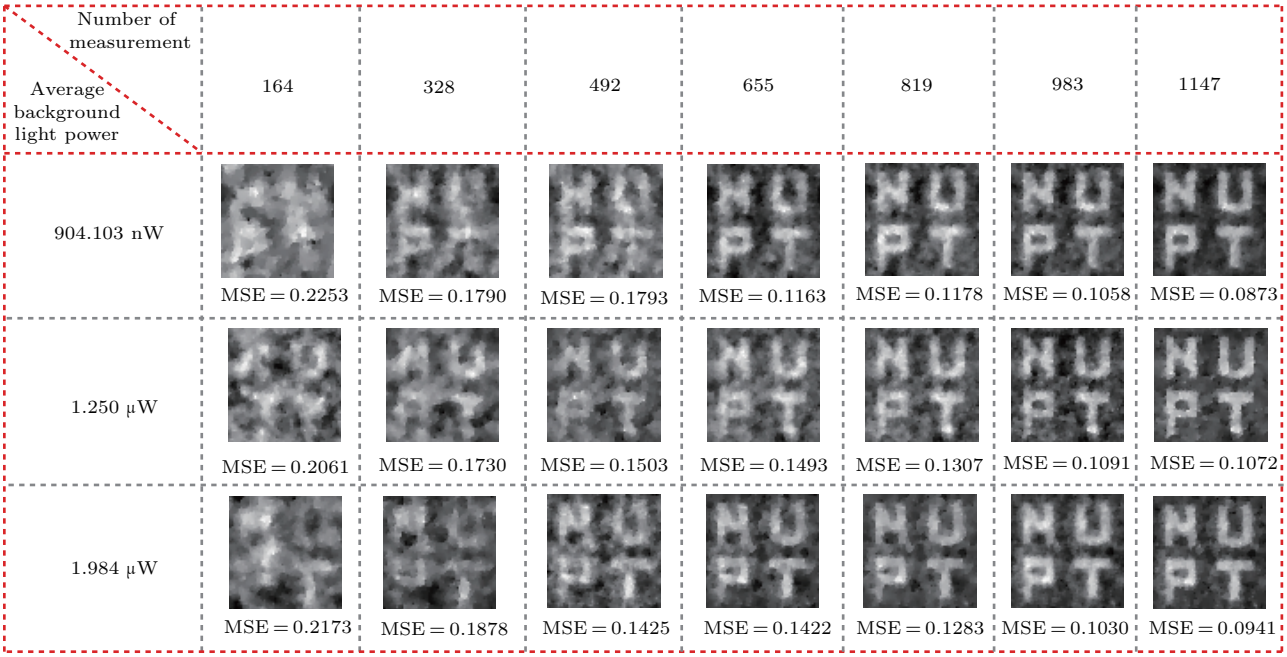


Fig. 8. The experimental results of the "NUPT" logo by using CCGI scheme, where MSE is presented together.

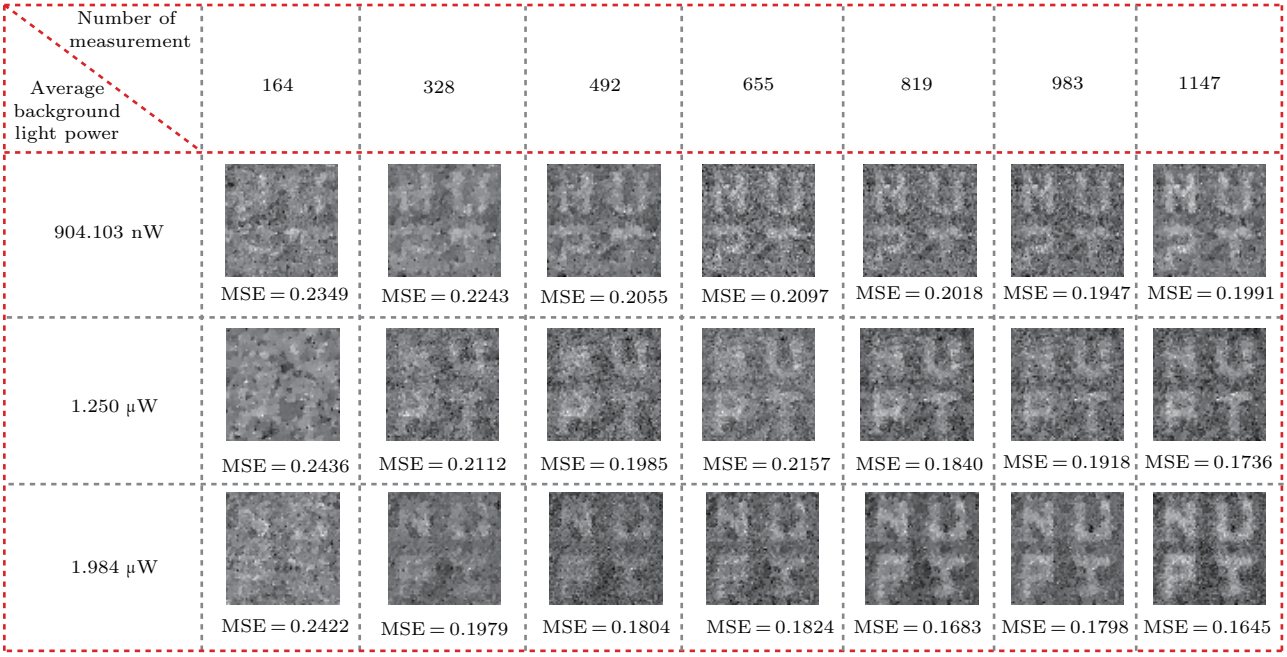


Fig. 9. The experimental results of the "NUPT" logo by using TCGI scheme, where MSE is presented together.

4. Conclusion

We have proposed a compressed ghost imaging scheme based on differential speckle patterns (CGI-DSP) in this paper. We have verified the feasibility of CGI-DSP by simulations and experiments. Moreover, we have compared the performance of CGI-DSP, CCGI, and TCGI. The results show that CGI-DSP can improve the imaging quality and decrease the number of measurements comparing with TCGI and CCGI.

References

[1] Strekalov D V, Sergienko A V, Klyshko D N and Shih Y H 1995 *Phys. Rev. Lett.* **74** 3600

[2] Bennink R S, Bentley S J and Boyd R W 2002 *Phys. Rev. Lett.* **89** 113601

[3] Cao D Z, Xu B L, Zhang S H and Wang K G 2015 *Chin. Phys. Lett.* **32** 114208

[4] Li H X, Bai Y F, Shi X H, Nan S Q, Qu L J, Shen Q and Fu X Q 2017 *Chin. Phys. B* **26** 104204

[5] Wang L, Zou L and Zhao S 2018 *Opt. Commun.* **407** 181

[6] Yin M Q, Wang L and Zhao S M 2019 *Chin. Phys. B* **28** 094201

[7] Liu J, Wang J, Chen H, Zheng H, Liu Y, Zhou Y, Li F and Xu Z 2018 *Opt. Commun.* **410** 824

[8] Katz O, Bromberg Y and Silberberg Y 2009 *Appl. Phys. Lett.* **95** 131110

[9] Candès E J, Romberg J K and Tao T 2006 *Commun. Pur. Appl. Math.* **59** 1207

[10] Sun M J, Meng L T, Edgar M P, Padgett M J and Radwell N A 2017 *Sci. Rep.* **7** 3464

[11] Gong W, Zhao C, Yu H, Chen M, Xu W and Han S 2016 *Sci. Rep.* **6** 26133

[12] Zhao S and Zhuang P 2014 *Chin. Phys. B* **23** 054203

[13] Zhao S, Wang L, Liang W, Cheng W and Gong L 2015 *Opt. Commun.* **353** 90

[14] Wang L, Zhao S, Cheng W, Gong L and Chen H 2016 *Opt. Commun.* **366** 314

[15] Yu W K, Yao X R, Liu X F, Li L Z and Zhai G J 2015 *Appl. Opt.* **54** 363

[16] Wang L and Zhao S 2016 *Photon. Res.* **4** 240

[17] Welsh S S, Edgar M P, Bowman R, Sun B and Padgett M J 2015 *J. Opt.* **17** 025705

[18] Li P, Hastie T J and Church K W 2006 *Proceedings of the 12th ACM SIGKDD international conference on Knowledge discovery and data mining*, August 20–23, 2006, Philadelphia, PA, USA, pp. 287–296

[19] Achlioptas D 2003 *J. Comput. Syst. Sci.* **66** 671

[20] Li C B 2010 *An efficient algorithm for total variation regularization with applications to the single pixel camera and compressive sensing* (Master Dissertation) (Houston: Rice University)